Published OnlineFirst November 3, 2015; DOI: 10.1158/0008-5472.CAN-15-0614

Cancer Research

Nrf2 Activation Promotes Keratinocyte Survival during Early Skin Carcinogenesis via Metabolic Alterations

Frank Rolfs[1], Marcel Huber[2], Andreas Kuehne[3], Stefan Kramer[1], Eric Haertel[1], Sukalp Muzumdar[1], Johanna Wagner[1], Yasmine Tanner[1], Friederike Böhm[4], Sigrun Smola[5], Nicola Zamboni[3], Mitchell P. Levesque[6], Reinhard Dummer[6], Hans-Dietmar Beer[6], Daniel Hohl[2], Sabine Werner[1], and Matthias Schäfer[1]

Abstract

Pharmacologic activation of the transcription factor NRF2 has been suggested to offer a strategy for cancer prevention. In this study, we present evidence from murine tumorigenesis experiments suggesting there may be limitations to this possibility, based on tumorigenic effects of Nrf2 in murine keratinocytes that have not been described previously. In this setting, Nrf2 expression conferred metabolic alterations in keratinocytes that were protumorigenic in nature, affecting enzymes involved in glutathione biosynthesis or in the oxidative pentose phosphate pathway and other NADPH-producing enzymes. Under stress conditions, coordinate increases in NADPH, purine, and glutathione levels promoted the survival of keratinocytes harboring oncogenic mutations, thereby promoting tumor development. The protumorigenic activity of Nrf2 in keratinocytes was particularly significant in a mouse model of skin tumorigenesis that did not rely upon chemical carcinogenesis. In exploring the clinical relevance of our findings, we confirm that NRF2 and protumorigenic NRF2 target genes were activated in some actinic keratoses, the major precancerous lesion in human skin. Overall, our results reveal an unexpected tumor-promoting activity of activated NRF2 during early phases of skin tumorigenesis. *Cancer Res; 75(22); 1–13. ©2015 AACR.*

Introduction

Epithelial skin cancers are the most frequent malignancies in humans. The continuous increase in their incidence is a consequence of the increasing life expectancy combined with UV light exposure. Reactive oxygen species (ROS) are important in this process, since they cause DNA damage and thereby promote malignant transformation (1).

To counteract the deleterious effects of ROS, cells have developed antioxidant defense strategies. Of particular importance is the transcription factor nuclear factor erythroid derived 2, like 2 (Nrf2), which regulates the expression of antioxidant proteins and enzymes involved in ROS or xenobiotic detoxification (2). Because of these important functions, loss of Nrf2 has detrimental consequences. In UV-irradiated Nrf2 knockout mice, ROS levels were increased, resulting in enhanced apoptosis (3, 4). Most importantly, these mice as well as mice expressing a dominant-negative Nrf2 mutant in keratinocytes showed increased susceptibility to skin carcinogenesis induced by the mutagen 7,12-dimethylbenz[*a*]anthracene (DMBA) and the tumor promoter 12-*O*-tetradecanoylphorbol 13-acetate (TPA; refs. 5, 6).

These results suggested that activation of Nrf2 is a promising strategy for skin cancer prevention. This can be achieved by various natural and synthetic compounds, which weaken the interaction of Nrf2 with the inhibitory protein kelch-like ECH-associated protein 1 (Keap1). Because Keap1 mediates Nrf2′s degradation via the ubiquitin-proteasome pathway, this causes Nrf2 stabilization and its accumulation in the nucleus (2). Genetic or pharmacologic Nrf2 activation in keratinocytes protected from UV-induced ROS damage and apoptosis, which is in line with a protective function of Nrf2 in the skin (3, 7, 8). Furthermore, Nrf2-activating compounds were shown to suppress tumorigenesis through their chemopreventive and anti-inflammatory activities (9). For example, treatment of mice with the Nrf2 activating compound sulforaphane reduced tumor incidence and multiplicity in the DMBA/TPA tumor model and protected against UV-induced carcinogenesis (5, 8). Nrf2-activating compounds are in preclinical and clinical trials for cancer prevention (9).

However, Nrf2 activation and antioxidants were shown to promote the malignancy of cells from established tumors and their radio- and chemotherapy resistance (9, 10). NRF2 activation in tumor cells occurs through mutations in the *NRF2* or *KEAP1* genes, transcriptional activation of the *NRF2* gene, epigenetic silencing of the *KEAP1* gene, or functional inhibition of the KEAP1

[1]Department of Biology, Institute of Molecular Health Sciences, ETH Zurich, Zurich, Switzerland. [2]Service de Dermatologie et Vénéréologie, Hôpital de Beaumont, Université de Lausanne, Lausanne, Switzerland. [3]Department of Biology, Institute for Systems Biology, ETH Zurich, Zurich, Switzerland. [4]Institute of Surgical Pathology, University Hospital Zurich, University of Zurich, Zurich, Switzerland. [5]Institute of Virology, Saarland University, Homburg, Germany. [6]Department of Dermatology, University Hospital Zurich, University of Zurich, Zurich, Switzerland.

Note: Supplementary data for this article are available at Cancer Research Online (http://cancerres.aacrjournals.org/).

Corresponding Authors: Matthias Schäfer, ETH Zurich, Institute of Molecular Health Sciences, Otto-Stern-Weg 7, 8093 Zurich, Switzerland. Phone: 41-44-633-3406; Fax: 41-44-633-1174; E-mail: matthias.schaefer@biol.ethz.ch; and Sabine Werner, E-mail: sabine.werner@biol.ethz.ch

doi: 10.1158/0008-5472.CAN-15-0614

Published OnlineFirst November 3, 2015; DOI: 10.1158/0008-5472.CAN-15-0614

protein (10). NRF2-activating mutations were detected in a variety of cancers (11), including 6% of human cutaneous squamous cell carcinomas (12). These data suggest that the consequences of NRF2 activation critically depend on the stage of tumorigenesis: it inhibits the initiation of tumor formation by preventing DNA damage, but enhances proliferation and chemoresistance of cancer cells.

Because there is little information on the role and mechanism of action of Nrf2 in the early phase of tumor promotion (9) and to specifically address the role of Nrf2 in epithelial cells for carcinoma development, we analyzed the consequences of genetic activation of Nrf2 in keratinocytes for skin tumor formation. We demonstrate an unexpected tumor-promoting function of Nrf2 during early skin tumorigenesis.

Materials and Methods

Animal experiments

Transgenic mice expressing constitutively active Nrf2 (K5cre-caNrf2 mice) or the early genes of human papilloma virus type 8 in keratinocytes (K14-HPV8 mice) were previously described (3, 13). caNrf2 mice were crossed with K14-HPV8 mice (both in FVB/N background). The double transgenic progeny was mated with K5cre mice in C57BL/6 background. Mice resulting from this breeding were observed bi-weekly for skin tumors. They were euthanized according to animal welfare regulations when a single tumor had a diameter of more than 1 cm, when more than one tumor of >0.5 cm appeared or when a tumor had an unfavorable localization.

For chemical carcinogenesis, back skin of 12- to 13-week-old female mice was shaved and 2 days later 25 μg DMBA in 200 μL acetone (Sigma) was applied topically. One week later, 5 μg TPA (Sigma) in 200 μL acetone was applied to the same site once weekly for 34 weeks. Tumor number and size were documented bi-weekly.

Mice were anaesthetized by intraperitoneal injection of xylazine/ketanarkon (Streuli Pharma AG) and sacrificed by CO_2 inhalation.

Cell culture

The murine 308 keratinocyte cell line was obtained from Cell Lines Service, where it had been tested for sterility using DAPI staining and mycoplasma PCR (http://www.clsgmbh.de/pdf/kera-308.pdf). Cells were used within the first 3 months after receipt. Murine primary keratinocytes were isolated from skin of newborn or 8 to 10 weeks old adult mice (14) and cultured in defined keratinocyte serum-free medium (Life Technologies).

Human foreskin keratinocytes were cultured in keratinocyte-serum-free medium and murine 308 keratinocytes (Cell Lines Service) in DMEM (Sigma) with 10% FCS in 6-well plates. At 60% confluency, cells were treated with 5 μmol/L sulforaphane (Enzo Life Sciences) overnight, and subsequently with 100 nmol/L TPA (Sigma), 12.5 μmol/L or 25 μmol/L menadione (Sigma), 50 μmol/L, 250 μmol/L or 500 μmol/L dehydroepiandrosterone (DHEA; Sigma), or 700 μmol/L 6-aminonicotinamide (6AN; Sigma) for 6–24 h.

Metabolomic analysis

Metabolites from frozen 70 to 90 mg mouse epidermis were extracted with 4 mL 70% ethanol at 75°C for 2 minutes followed by 90-second sonication. After centrifugation at 2,900 g for 10 minutes at 4°C, supernatants were dried at 0.12 mbar pressure and resuspended with nanopure water. Quantitative targeted analysis of selected metabolites was performed using ultra high-pressure liquid chromatography-coupled tandem mass spectrometry (15). Untargeted metabolite profiling was conducted by flow-injection analysis on an Agilent 6550 Q-TOF (Agilent) in negative mode, 4 GHz high-resolution mode, scanning the m/z range of 50 to 1,000 (16). Ions were annotated to known metabolites based on exact mass with a tolerance of 0.001 Da and considering $[M\text{-}H^+]$ and $[M+F^-]$ ions using the HMDB v3.0 database (17). Differences in metabolic pathways were identified using a hypergeometric test on significantly changing metabolites [P value < 0.01, $|\log_2(\text{fold change})| > 0.2$, and limited to the 50 most significant hits ranked by fold change]. The analysis was performed recursively for each pathway by first considering only the most significant metabolite as hit, and then increasing with each iteration the hit subset with the next most changing metabolite. The best P value of this recursive analysis represents the probability of metabolic enrichment for a given pathway. Data analysis was performed using Matlab 2014a (The Mathworks).

Morphometrical and statistical analysis

Skin samples or cultured cells were photographed, and cell number, epidermal length, or area was analyzed using Open Lab software 3.1.5 (Improvision/PerkinElmer), omitting hair follicles.

Statistical analysis was performed using Prism 5 Software (GraphPad Software Inc.). Tumor incidence (HPV8 model) was analyzed using log-rank (Mantel-Cox) test, metabolic pathway enrichment using Fisher exact test. For comparison of two groups of data, Mann–Whitney U test was used. Error bars represent SD in all graphs. *, $P \leq 0.05$; **, $P \leq 0.01$; ***, $P \leq 0.001$.

Study approval

All animal experiments had been approved by the local veterinary authorities of Zurich or Lausanne, Switzerland.

Human skin biopsies were obtained from the Department of Dermatology, University Hospital Zurich (Zurich, Switzerland), as part of the University Research Priority Program in Translational Cancer Research Biobank project, approved by the local and cantonal Institution Review Boards EK no. 647 and 800. Written informed consent was received from all patients. All research on human material abided by the Helsinki Declaration on Human Rights.

Results

Nrf2 activation has a mild tumor-preventive effect in a model of chemically induced skin carcinogenesis

To analyze the consequences of Nrf2 activation in keratinocytes on skin tumorigenesis, we used mice expressing a constitutively active Nrf2 (caNrf2) mutant in all keratinocytes due to Cre-mediated excision of a floxed STOP cassette in basal cells of the epidermis and in outer root sheath keratinocytes of hair follicles (K5cre-caNrf2 mice; ref. 3). These mice showed low mRNA levels of the transgene in keratinocytes comparable with endogenous *Nrf2*. Expression of classical Nrf2 target genes was significantly upregulated. Nevertheless, they do not have obvious abnormalities in the back skin (14).

K5cre-caNrf2 mice were subjected to a DMBA/TPA-induced skin carcinogenesis protocol (18). Expression of *caNrf2* and upregulation of the Nrf2 target genes NAD(P)H dehydrogenase, quinone 1 (*Nqo1*) and glutathione S-transferase A3 (*Gsta3*) were confirmed after short- and long-term TPA treatment

Published OnlineFirst November 3, 2015; DOI: 10.1158/0008-5472.CAN-15-0614

(Supplementary Fig. S1A and S1B). Surprisingly, tumor incidence and multiplicity were only slightly reduced in K5cre-caNrf2 compared with controls, and malignant progression and histopathological features were not affected (Fig. 1A–D). Some K5cre-caNrf2 mice developed sebaceous adenomas (Fig. 1D and Supplementary Fig. S1C), consistent with the enlarged sebaceous glands in mice with stronger Nrf2 activation (3, 19).

Nrf2 activation enhances DMBA and ROS detoxification

To determine whether the mild tumor-suppressive effect of caNrf2 results from enhanced DMBA and/or ROS detoxification, we used RNA from skin of untreated K5cre-caNrf2 and control mice at postnatal day 2.5 (P2.5) for RNA profiling. Expression of enzymes involved in detoxification of benzo[a]pyrene and/or DMBA was strongly induced by caNrf2 (Supplementary Table S1

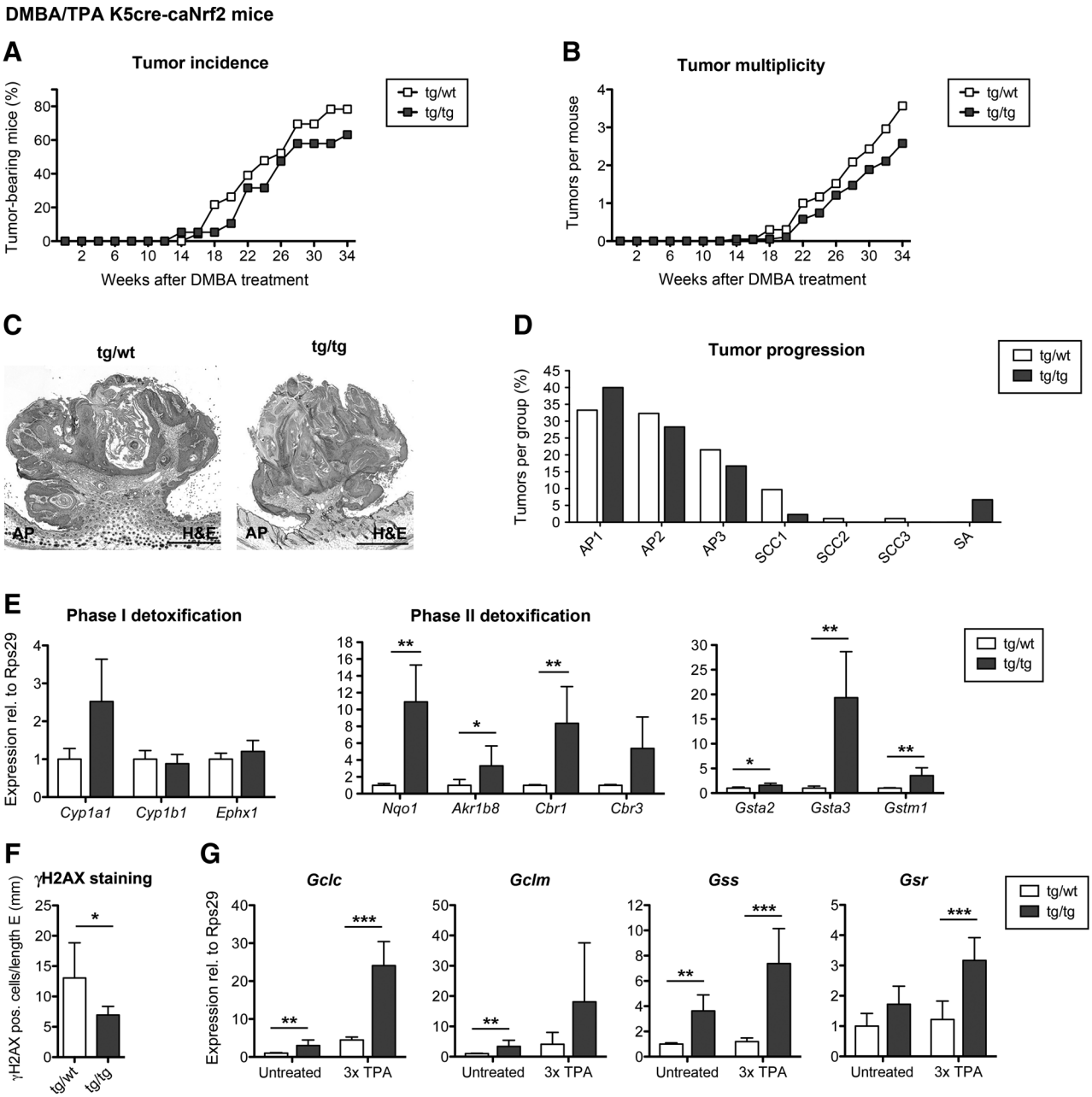

Figure 1.

Reduced DMBA/TPA-induced skin tumorigenesis in K5cre-caNrf2 mice. A and B, tumor incidence (A) and multiplicity (B) in K5cre-wt (tg/wt; $N = 23$) and K5cre-caNrf2 mice (tg/tg; $N = 19$). C, H&E staining of representative acanthopapillomas (AP). Scale bar, 1 mm. D, histopathological classification of tumors from tg/wt ($N = 22$; $n = 93$) and tg/tg ($N = 20$; $n = 60$) mice. The percentage of acanthopapillomas stage I–III, squamous cell carcinomas (SCC) stage I–III, and sebaceous adenomas (SA) is shown. E, qRT-PCR for *Cyp1a1*, *Cyp1b1*, *Ephx1*, *Nqo1*, *Akr1b8*, *Cbr1*, *Cbr3*, *Gsta2*, *Gsta3*, and *Gstm1* relative to *Rps29* using RNA from untreated tg/wt and tg/tg mice. Mean values of tg/wt mice were set to 1. $N = 4/6$. F, number of γH2AX-positive cells per length epidermis. $N = 7$. G, qRT-PCR for *Gclc*, *Gclm*, *Gss*, and *Gsr* relative to *Rps29* using RNA from untreated and 3× TPA-treated tg/wt and tg/tg mice. Untreated $N = 4/6$, 3× TPA $N = 8/7$.

Published OnlineFirst November 3, 2015; DOI: 10.1158/0008-5472.CAN-15-0614

and Supplementary Fig. S1D; refs. 20, 21). This was confirmed by qRT-PCR for *Nqo1*, aldo-keto reductase (*Akr*)*1b8*, carbonyl reductases (*Cbr*)1 and *Cbr3*, and for *Gsta2*, *Gsta3* and *Gstm1* in the epidermis of untreated and 1× DMBA-treated mice (Fig. 1E and Supplementary Fig. S1E). Expression of the DMBA-activating enzyme cytochrome P450-1a1 (*Cyp1a1*) was also mildly increased. *Cyp1b1* and epoxide hydrolase 1 (*Ephx1*) expression was unaltered (Fig. 1E and Supplementary Fig. S1D). caNrf2 did also not affect the number of Langerhans cells (Supplementary Fig. S1F), the major cell type expressing DMBA-activating enzymes in the epidermis (22). IHC revealed a significant reduction of γH2AX-positive keratinocytes in 1× DMBA-treated K5cre-caNrf2 mice compared with control mice (Fig. 1F), demonstrating that Nrf2 activation protected from DMBA-induced DNA damage, most likely through upregulation of phase II-detoxifying enzymes (see working model Fig. 6G).

During chemical carcinogenesis, ROS are formed in the course of DMBA and TPA metabolism and inflammation, thus accelerating the accumulation of mutations (23). Indeed, expression of proinflammatory cytokines and the number of neutrophils strongly increased in response to TPA treatment, but to a similar extent in K5cre-caNrf2 and control mice (Supplementary Fig. S2A and S2B). However, thirty genes involved in ROS detoxification were more than 1.5-fold upregulated in K5cre-caNrf2 mice according to RNA profiling data (Supplementary Table S1). This was confirmed by qRT-PCR for *Gsta3*, *Nqo1* (Supplementary Fig. S1A and S1B), and for glutamate cysteine ligase catalytic subunit (*Gclc*) and modifier subunit (*Gclm*), glutathione synthetase (*Gss*) and glutathione reductase (*Gsr*) using RNAs from epidermis of untreated and 3× TPA-treated mice (Fig. 1G). These results suggest that Nrf2 activation also protects from ROS-induced DNA damage (see working model in Fig. 6G). In light of this finding, the relatively mild reduction of tumor incidence and multiplicity in K5cre-caNrf2 mice suggested a counteracting protumorigenic effect of activated Nrf2.

Nrf2 activation promotes HPV8-induced skin tumorigenesis

Because the effect of Nrf2 on DMBA and ROS detoxification could mask a possible tumor-promotive function of Nrf2 in skin carcinogenesis, we chose a tumor model that does not depend on chemical carcinogens. For this purpose, we mated K5cre-caNrf2 mice with K14-HPV8 transgenic mice, which develop spontaneous skin papillomas due to expression of the oncogenes *HPV8-E6* and *E7* in keratinocytes (13). HPV8 is associated with skin tumorigenesis in humans (24, 25).

Surprisingly, tumor development was strongly accelerated in K14-HPV8/K5cre-caNrf2 (tg/tg/tg) mice compared with K14-HPV8/K5cre-wt (control; tg/tg/wt) mice (Fig. 2A and B). Mice with large papillomas had to be eliminated, and the number of papillomas at the date of sacrifice was included in the graphs at all later time points (cumulative tumor multiplicity). Therefore, the differences between genotypes are most likely underestimated. Since only few K14-HPV8/K5cre-caNrf2 mice were still alive after 2 years, later time points were not included in the statistics. Although papillomas of K14-HPV8/K5cre-caNrf2 mice showed a significant increase in expression of *Nqo1* and *Gsta3* compared with tumors of control mice, there was no difference in the time intervals between the appearance of the first and the second papilloma, in the papilloma growth rate, in the age of papillomas at sacrifice, or in their localization (Supplementary Fig. S3A–S3E). Papillomas from mice of both genotypes showed similar histopathological features, and Nrf2 activation did not affect tumor progression (Fig. 2C and D).

Expression of the *HPV8-E6* oncogene was not affected by the *caNrf2* transgene (Fig. 2E), indicating that the enhanced tumorigenesis indeed results from upregulation of Nrf2 target genes. Proinflammatory cytokines were only weakly expressed in the skin of K14-HPV8 mice. However, local inflammation resulting from scratching was observed in some mice (Supplementary Fig. S4A–S4C), which most likely promotes tumor formation as previously seen in these mice after wounding (26). Inflammation was not obviously affected by the *caNrf2* transgene (Supplementary Fig. S4D–S4F). However, a significant increase in the expression of enzymes involved in ROS defense was detected (Fig. 2F and G), suggesting that Nrf2 activation also reduced oxidative stress in K14-HPV8 mice, which is relevant at the site of inflammation (see working model; Fig. 6H). These results raise the question how Nrf2 activation enhances tumor formation in K14-HPV8 transgenic mice.

Nrf2 activation in keratinocytes causes metabolic alterations

To unravel the mechanisms underlying the protumorigenic effect of caNrf2, we performed mass spectrometry-based untargeted metabolomic analysis (16) using epidermis of K5cre-caNrf2 and control mice after three TPA treatments. We found significant Nrf2-mediated alterations in pathways of glutathione (***, $P = 2 \times 10^{-6}$) and purine metabolism (***, $P = 2 \times 10^{-4}$) and in amino acid metabolism pathways (Fig. 3A). Levels of reduced and oxidized glutathione (GSH and GSSG) were strongly elevated in K5cre-caNrf2 mice, and a mild increase in the GSH precursors glycine, cysteine, and glutamate was observed (Fig. 3B and Supplementary Fig. S5A). ATP and GTP levels were increased, whereas levels of uric acid, an intermediate in purine degradation, were decreased (Fig. 3C).

Untargeted metabolomic analysis of epidermis from K14-HPV8/K5cre-caNrf2 and control mice revealed similar changes in glutathione and purine metabolism (Fig. 3D and E). However, GSSG was not increased, reflecting only limited oxidative stress compared with DMBA/TPA-treated K5cre-caNrf2 mice. Targeted metabolomic analysis furthermore revealed enhanced levels of metabolites of the pentose phosphate pathway (PPP), the citric acid cycle, glycolysis, and purine synthesis (Supplementary Fig. S5A–S5C).

Nrf2 activation enhances expression of enzymes involved in glutathione and NADPH production in keratinocytes

The increase in GSH in the epidermis of caNrf2 transgenic mice can be explained by upregulation of *Gclc*, *Gclm*, *Gss*, and *Gsr* (Figs. 1G and 2G), of the cystine/glutamate transporter *Slc7a11*, and of the neutral amino acid transporter *Slc1a4* (Supplementary Table S1). Purines are synthesized from glucose through the PPP and by purine biosynthesis enzymes (Supplementary Fig. S5A). A significant upregulation of the oxidative PPP enzymes glucose-6-phosphate dehydrogenase X-linked (G6pdx) and phosphogluconate dehydrogenase (Pgd) was detected in P2.5 K5cre-caNrf2 mice by microarray analysis, whereas expression of genes encoding glycolytic enzymes was normal (Supplementary Tables S1 and S2). qRT-PCR and Western blot analyses confirmed upregulation of G6pdx, Pgd, transketolase (Tkt), and transaldolase 1 (Taldo1) in the epidermis of untreated and 3× TPA-treated adult K5cre-caNrf2 mice (Fig. 4A

Published OnlineFirst November 3, 2015; DOI: 10.1158/0008-5472.CAN-15-0614

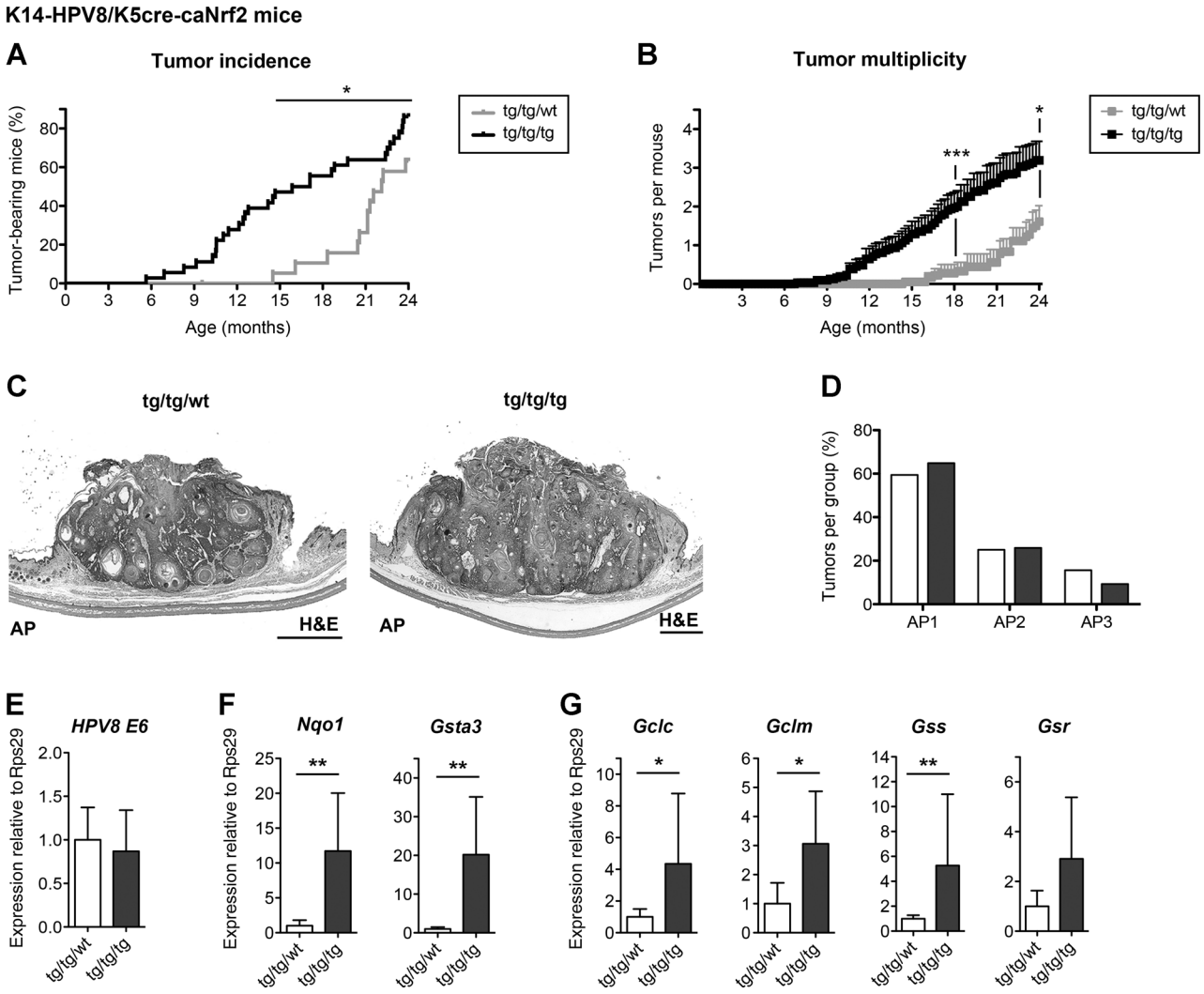

Figure 2.

Enhanced skin tumorigenesis and ROS detoxification in K14-HPV8/K5cre-caNrf2 mice. A and B, tumor incidence (A) and cumulative tumor multiplicity (B) in K14-HPV8/K5cre-wt (tg/tg/wt) mice and K14-HPV8/K5cre-caNrf2 (tg/tg/tg) mice. Tumor incidence, $N = 20$–36; tumor multiplicity, $N = 19$-29/19-36. C, H&E staining of representative acanthopapillomas (AP). Scale bar, 1 mm. D, histopathological classification of acanthopapillomas from tg/tg/wt ($N = 19$; $n = 64$) and tg/tg/tg ($N = 30$; $n = 108$) mice. The percentage of acanthopapillomas at stages I–III among all skin lesions is indicated. E, qRT-PCR for *HPV8-E6* relative to *Rps29* using epidermal RNA from tg/tg/wt and tg/tg/tg mice. $N = 6$. F and G, qRT-PCR for *Nqo1* and *Gsta3* (F) and *Gclc*, *Gclm*, *Gss*, and *Gsr* (G) relative to *Rps29* using epidermal RNA from tg/tg/wt and tg/tg/tg mice. $N = 6$. Mean expression levels in tg/tg/wt mice were set to 1.

and B). These data strongly suggest that Nrf2 activation in keratinocytes increases the flux through the PPP, which is indirectly responsible for the elevated purine levels. Activities of G6pdx, Pgd, malic enzyme 1 (Me1), and isocitrate dehydrogenase 1 (Idh1) result in NADPH generation (Supplementary Fig. S5A), and *Me1* and *Idh1* expression was also significantly higher in the epidermis of K5cre-caNrf2 mice (Fig. 4C).

Upregulation of *G6pdx*, *Pgd*, *Taldo1*, *Tkt*, *Me1*, and *Idh1* was also observed in K14-HPV8/K5cre-caNrf2 mice, leading to increased levels of NADPH as revealed by targeted metabolomic analysis (Fig. 4D–F). Concomitantly, there was a reduction in the Idh1 substrate (iso)citrate and an increase in its product α-ketoglutarate (Supplementary Fig. S5D).

Treatment of primary keratinocytes with sulforaphane, which activated Nrf2 as shown by elevated expression of *Nqo1* and *Srxn1*, also caused a significant upregulation of *G6pdx*, *Pgd*, *Taldo1*, *Tkt*, *Idh1*, and *Me1* (Fig. 4G–J). This indicates that these genes are under direct control of Nrf2 in murine keratinocytes. In contrast, the increased expression of these genes and the concomitant metabolic alterations are unlikely to result from activation of NFκB in response to Nrf2 activation. NFκB signaling plays a crucial role in skin tumor formation (27–30). However, microarray analysis using RNA from back skin of P2.5 K5cre-caNrf2 mice revealed no significant regulation of NFκB target genes, except for *Nqo1*, which is also a major Nrf2 target gene (Supplementary Fig. S6A). Furthermore, expression of baculoviral IAP repeat containing 3 (*Birc3*) and TNFα-induced protein 3 (*Tnfaip3*), key driver genes in NFκB-p65–dependent skin tumor formation (27), was unaffected in the epidermis of 3× TPA-treated K5cre-caNrf2 mice and only slightly downregulated in the epidermis of K14-HPV8/K5cre-caNrf2 mice (Supplementary Fig. S6B and S6C).

Published OnlineFirst November 3, 2015; DOI: 10.1158/0008-5472.CAN-15-0614

Taken together, genetic Nrf2 activation in keratinocytes directly increases NADPH and ATP synthesis, which are required for GSH synthesis/recycling and DMBA detoxification (Supplementary Figs. S1D and S5A).

Nrf2 activation does not affect keratinocyte proliferation

Surprisingly, the enhanced levels of NADPH, GSH, and ATP in K5cre-caNrf2 mice did not affect epidermal thickness and keratinocyte proliferation after TPA treatment (Fig. 5A and B). Moreover, expression of the cell-cycle regulators cyclin b1 (*Cncb1*) and aurora kinase b (*Aurkb*; Supplementary Fig. S7A), and activation of the mitogenic Erk and Akt signaling pathways were not affected (Fig. 5C).

There was also no effect on proliferation of keratinocytes with an oncogenic mutation as seen in 1× DMBA- and DMBA/TPA-treated K5cre-caNrf2 mice (Supplementary Fig. S7B and S7C) or

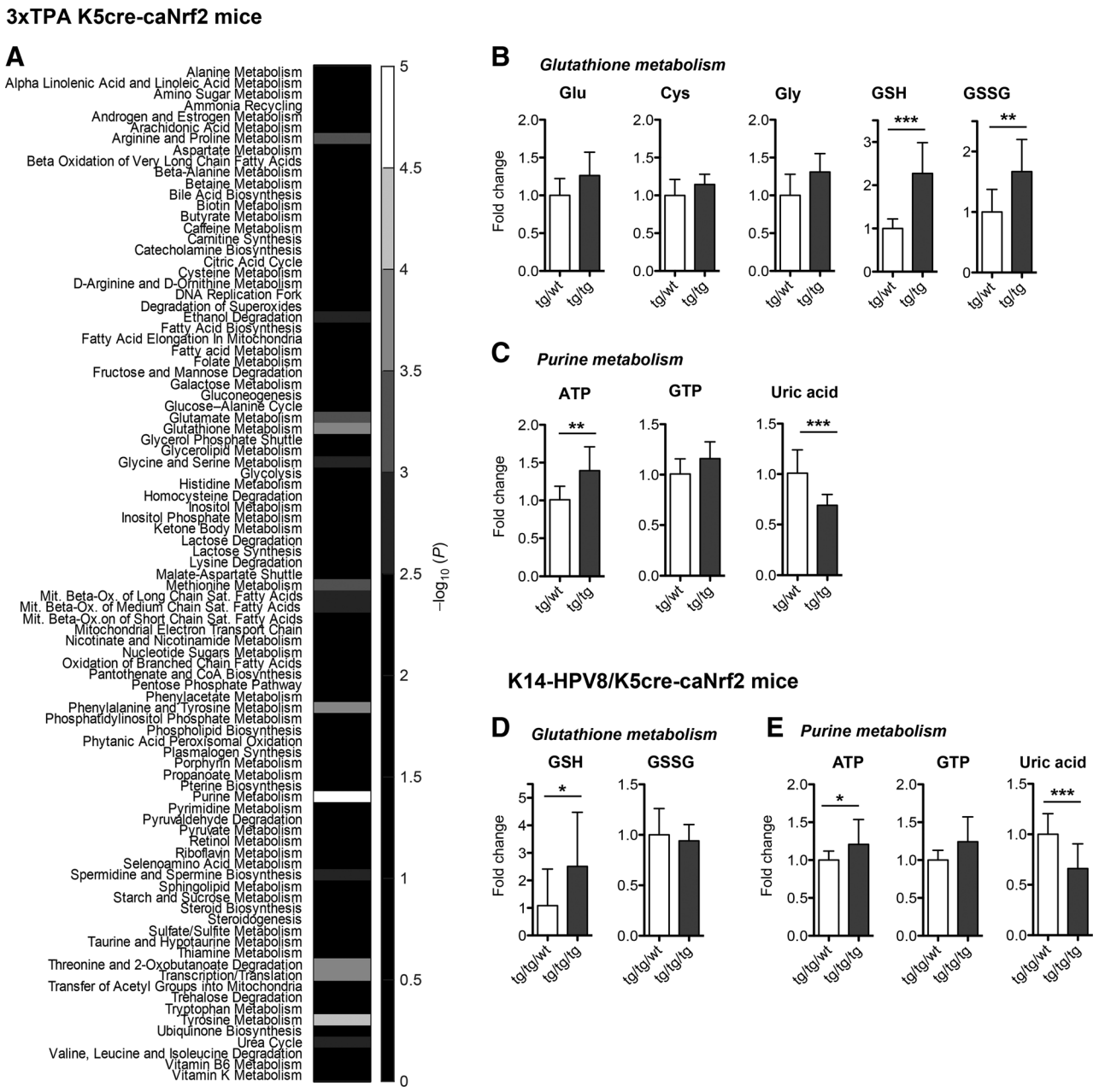

Figure 3.

Metabolomic alterations in the epidermis of TPA-treated K5cre-caNrf2 and K14-HPV8/K5cre-caNrf2 mice. A, heatmap showing enrichment of metabolic pathways as detected by untargeted metabolomic analysis of epidermis from 3× TPA-treated control (tg/wt) and K5cre-caNrf2 (tg/tg) mice. B and C, fold-change levels of metabolites of glutathione (B) and purine metabolism (C) in epidermis of 3× TPA-treated tg/wt compared with tg/tg mice. $N = 9/5$ animals, $N = 18/10$ samples. D and E, fold change in the levels of glutathione (D) and purine metabolism (E) in the epidermis of control (tg/tg/wt) and K14-HPV8/K5cre-caNrf2 (tg/tg/tg) mice, determined by untargeted metabolomic analysis. $N = 9/5$, $N = 18/10$ samples.

Published OnlineFirst November 3, 2015; DOI: 10.1158/0008-5472.CAN-15-0614

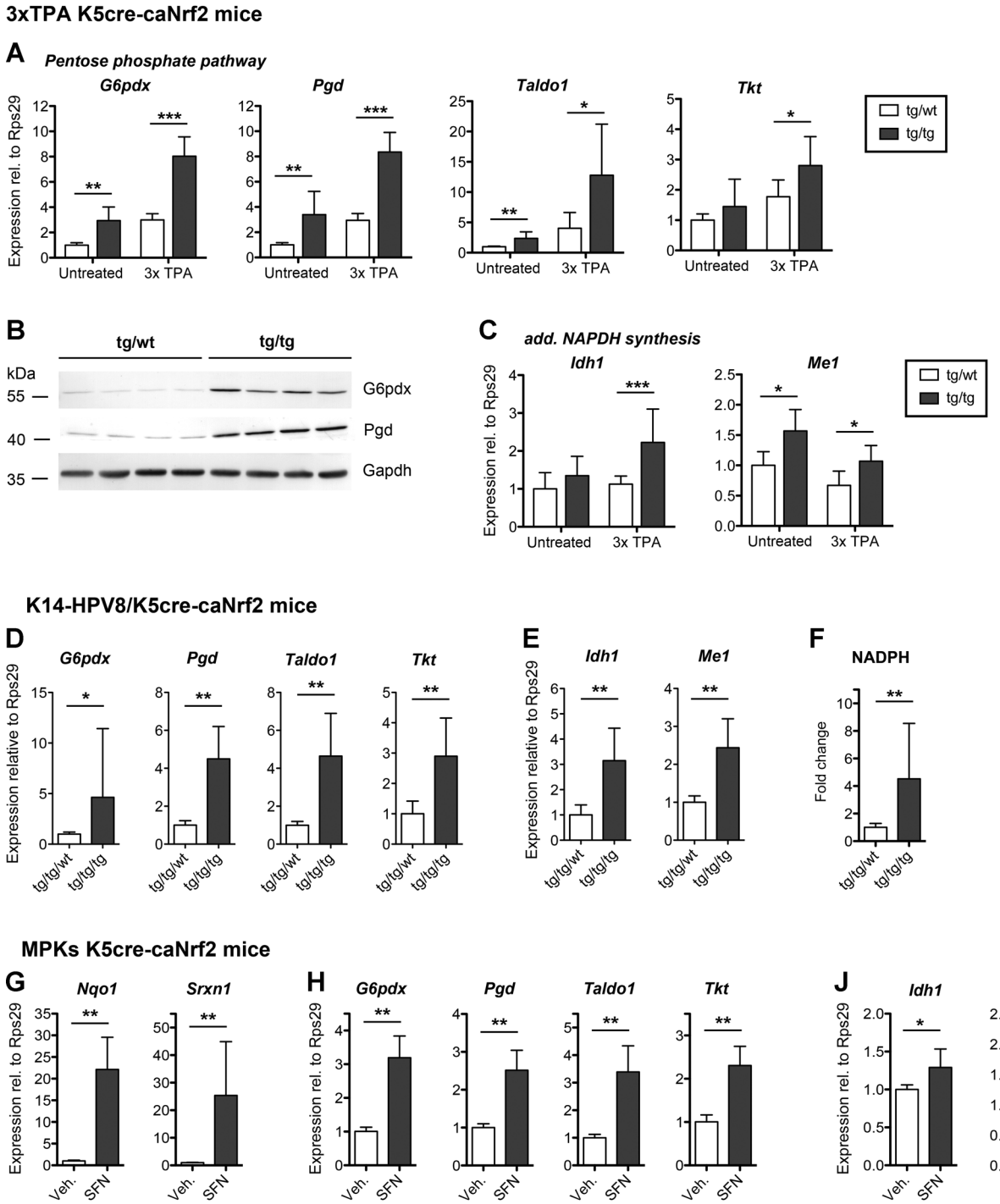

Figure 4.

Gene expression and metabolites in the epidermis of TPA-treated K5cre-caNrf2 and K14-HPV8/K5cre-caNrf2 mice. A and B, qRT-PCR for *G6pdx*, *Pgd*, *Taldo1*, and *Tkt* relative to *Rps29* (A) and Western blot analysis for Pgd, G6pdx, and Gapdh (B) using epidermis of untreated and 3× TPA-treated control (tg/wt) and K5cre-caNrf2 (tg/tg) mice. Untreated $N = 4/6$; 3× TPA $N = 8/7$. C, qRT-PCR for *Idh1* and *Me1* relative to *Rps29* using epidermal RNA from untreated and 3× TPA-treated tg/wt and tg/tg mice. Untreated $N = 4/6$; 3x TPA $N = 8/7$. D and E, qRT-PCR for *G6pdx*, *Pgd*, *Taldo1*, and *Tkt* (D) and *Me1* and *Idh1* (E) relative to *Rps29* using epidermal RNA from epidermis of control (tg/tg/wt) and K14-HPV8/K5cre-caNrf2 (tg/tg/tg) mice. $N = 6$. F, fold change in the levels of NADPH between epidermis of tg/tg/tg and tg/tg/wt mice, determined by targeted metabolomic analysis. $N = 6/5$. G–J, qRT-PCR for *Nqo1*, *Srxn1* (G), *G6pdx*, *Pgd*, *Taldo1*, *Tkt* (H), *Idh1*, and *Me1* (J) relative to *Rps29* using RNA from vehicle (Veh) or 5 μmol/L sulforaphane (SFN)-treated mouse primary keratinocytes (murine primary keratinocytes). Mean values of vehicle-treated murine primary keratinocytes were set to 1.

Published OnlineFirst November 3, 2015; DOI: 10.1158/0008-5472.CAN-15-0614

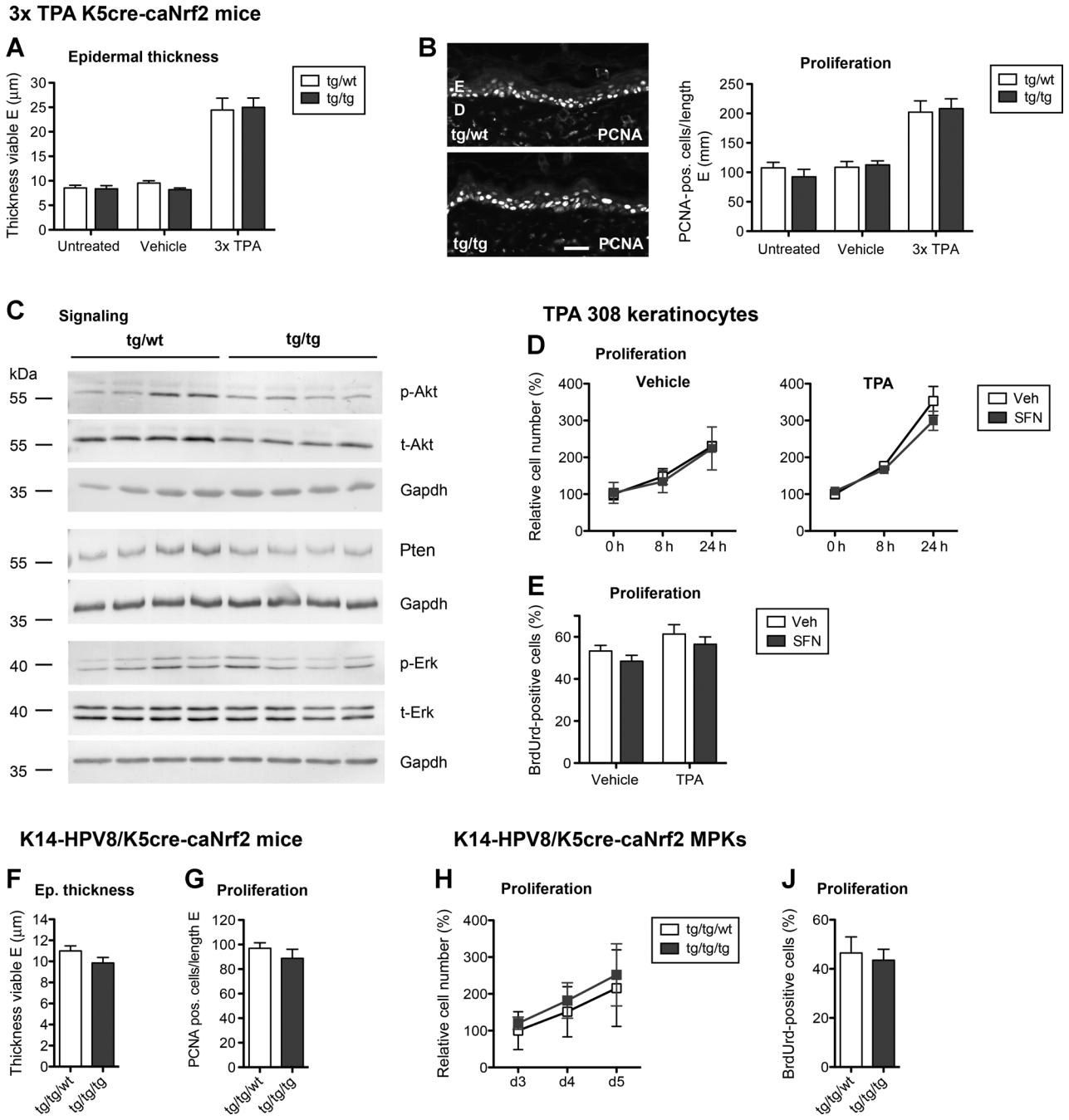

Figure 5.

Nrf2 activation does not affect keratinocyte proliferation. A, thickness of the viable epidermis of untreated ($N = 5$), 3× vehicle ($N = 5$), and 3× TPA-treated ($N = 6/7$) tg/wt and tg/tg mice. B, immunofluorescence staining for PCNA using sections from untreated, 3× vehicle-treated, and 3× TPA-treated tg/wt and tg/tg mice. Left, representative picture of 3× TPA-treated skin. Scale bar, 30 μm. Right, number of PCNA-positive cells per length epidermis. Untreated, $N = 3$; vehicle, $N = 4/3$; 3× TPA, $N = 4$. E, epidermis; D, dermis. C, Western blot analysis for phospho-Akt (p-Akt), total Akt (t-Akt), Pten, p-Erk, t-Erk, and Gapdh using protein lysates from tg/wt and tg/tg epidermis. D, total cell number per microscopic field of 5 μmol/L sulforaphane (SFN) or vehicle-treated 308 keratinocytes at 0, 8, and 24 hours after vehicle (left) or 100 nmol/L TPA treatment (right). $N = 6$. E, BrdUrd-positive cells per microscopic field of vehicle or sulforaphane and vehicle or TPA-treated 308 keratinocytes. $N = 6$. F and G, thickness of the viable epidermis (F) and number of PCNA-positive cells per length epidermis (G) of K14-HPV8/K5cre-wt (tg/tg/wt) and K14-HPV8/K5cre-caNrf2 (tg/tg/tg) mice. $N = 3$. H and J, total cell number at d3-5 after seeding (H) and number of PCNA-positive cells at d5 after seeding (J) per microscopic field of murine primary keratinocytes isolated from tg/tg/wt and tg/tg/tg mice. $N = 5$.

upon pharmacologic activation of Nrf2 by sulforaphane in TPA-treated 308 keratinocytes, which have an activating *h-ras* mutation (31, 32). Although sulforaphane significantly increased expression of genes involved in the control of the cellular redox balance and in the PPP in 308 keratinocytes (Supplementary Fig. S7D–S7F), it did not affect cell proliferation (Fig. 5D and E).

Published OnlineFirst November 3, 2015; DOI: 10.1158/0008-5472.CAN-15-0614

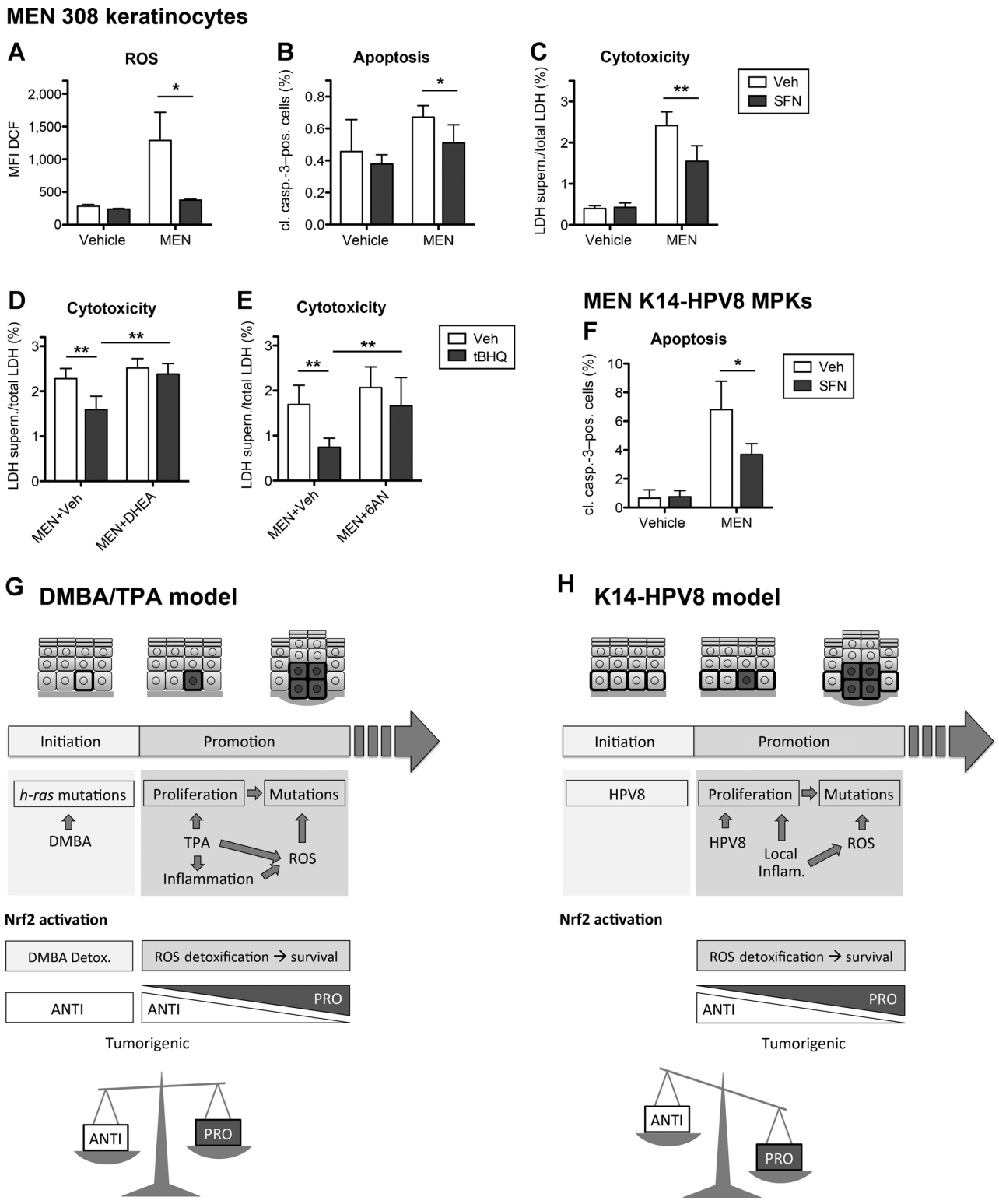

Figure 6.

Nrf2 activation inhibits ROS-induced damage and apoptosis of keratinocytes. A–C, median fluorescence intensity (MFI) of DCF (A), percentage of cleaved caspase-3–positive cells per microscopic field (B), and ratio of supernatant to total LDH activity (C) of 308 keratinocytes treated with 5 μmol/L sulforaphane (SFN) or vehicle and 25 μmol/L menadione (MEN) or vehicle. $N = 6/3$ (A); $N = 6$ (B and C). D and E, ratio of supernatant to total LDH activity of 308 keratinocytes treated with 50 μmol/L tBHQ or vehicle, 25 μmol/L menadione, and 700 μmol/L DHEA or vehicle (D), or 250 μmol/L 6AN or vehicle (E). $N = 6$. F, primary keratinocytes (murine primary keratinocytes) from K14-HPV8 transgenic mice treated with 5 μmol/L sulforaphane or vehicle and 25 μmol/L menadione or vehicle. The percentage of cleaved caspase-3–positive cells per microscopic field is shown. $N = 5$. G, working model of Nrf2 activation in DMBA/TPA-treated mice: the antitumorigenic Nrf2 activities counterbalance the protumorigenic Nrf2 activities, resulting in a slight reduction in tumor incidence (indicated by balance in the bottom panel). H, working model of Nrf2 activation in K14-HPV8 transgenic mice: the protumorigenic Nrf2 activities dominate over the antitumorigenic activities, resulting in enhanced tumorigenesis (indicated by balance in the bottom panel).

Published OnlineFirst November 3, 2015; DOI: 10.1158/0008-5472.CAN-15-0614

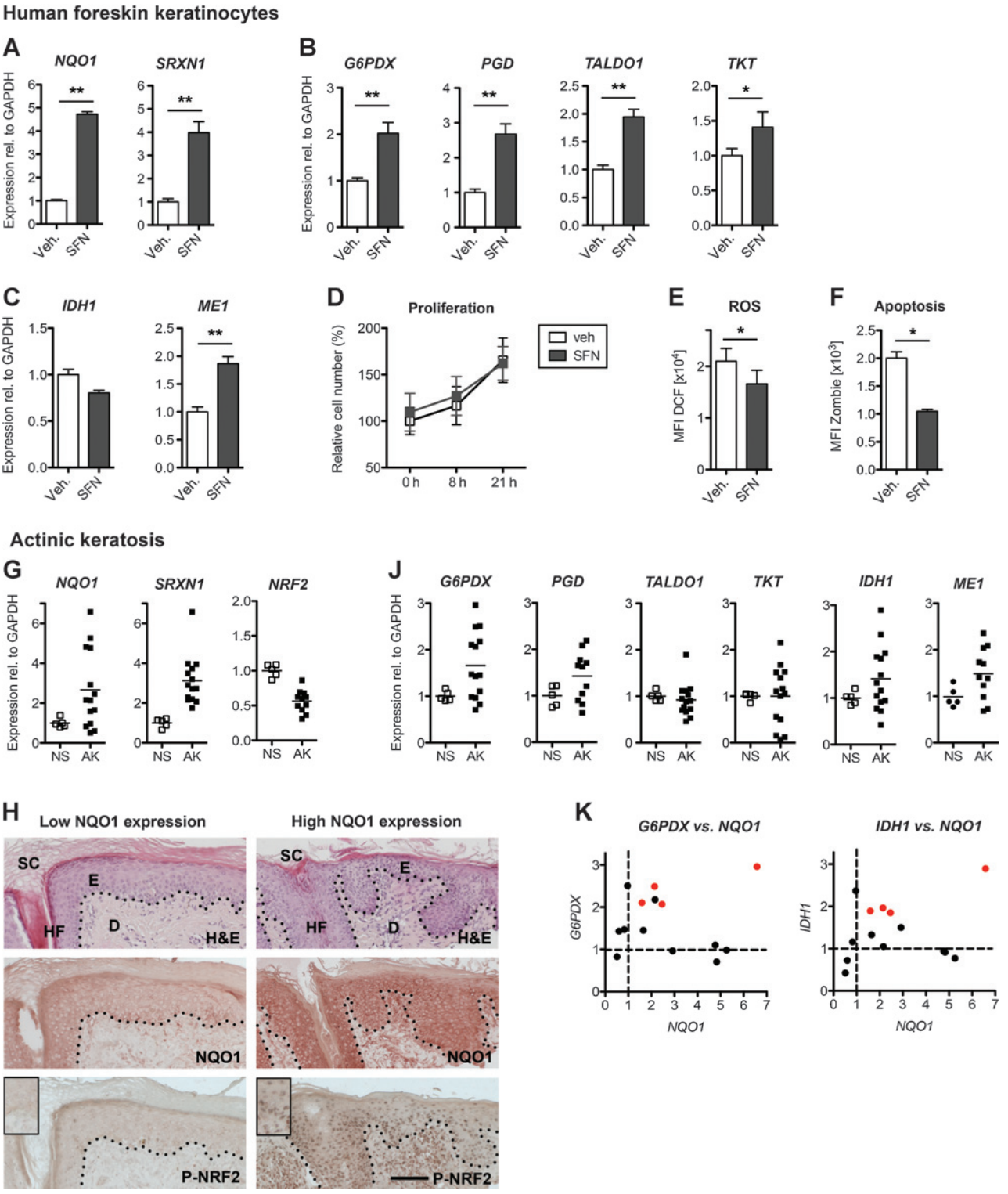

Figure 7.

NRF2 activation in primary human keratinocytes and in precursor lesions of human epithelial skin cancer. A–C, qRT-PCR for *NQO1, SRXN1* (A), *G6PDX*, *PGD*, *TKT*, *TALDO1* (B), *IDH1*, and *ME1* (C) relative to *GAPDH* using RNA from primary human foreskin keratinocytes treated with vehicle or 5 μmol/L sulforaphane (SFN). Mean values of vehicle-treated keratinocytes were set to 1. $N = 6$. D, total human foreskin keratinocyte number per microscopic field at 0, 6, and 21 hours after treatment with vehicle or 5 μmol/L sulforaphane. $N = 6$. E and F, median fluorescence intensity (MFI) of DCF (E) and of Zombie (F) in human foreskin keratinocytes treated with 5 μmol/L sulforaphane or vehicle. $N = 6$. G, qRT-PCR for *NQO1*, *SRXN1*, and *NRF2* relative to *GAPDH* using RNA from skin of healthy donors ($N = 5$ biopsies) and from patients with epithelial skin cancer precursor lesions ($N = 11/14$ biopsies; Supplementary Table S3). (*Continued on the following page.*)

Published OnlineFirst November 3, 2015; DOI: 10.1158/0008-5472.CAN-15-0614

K14-HPV8 single-transgenic mice also showed no change in epidermal thickness and keratinocyte proliferation (Supplementary Fig. S8A and S8B), and caNrf2 did not affect these parameters (Fig. 5F and G). Finally, primary keratinocytes from K14-HPV8/K5cre-caNrf2 mice and control mice had a similar proliferation rate (Fig. 5H and J).

A contribution of altered keratinocyte differentiation to the protumorigenic effect of caNrf2 was also excluded, since the differentiation markers loricrin, K10, and K14 were normally expressed in TPA-treated K5cre-caNrf2 mice, SNF-treated 308 keratinocytes and in K14-HPV8/K5cre-caNrf2 mice (Supplementary Fig. S8C–S8E).

Nrf2 activation enhances survival of premalignant cells

Keratinocytes with an *h-ras* mutation have increased ROS levels, resulting in enhanced apoptosis (33, 34). This, together with inflammation, leads to elimination of premalignant cells in the early phase of tumorigenesis. Nrf2 activation could promote the survival of cells in premalignant lesions by preventing ROS-induced apoptosis. Indeed, a mild reduction in the number of apoptotic cells was seen in the epidermis of DMBA/TPA-treated K5cre-caNrf2 mice and after sulforaphane treatment of 308 cells in the presence or absence of TPA (Supplementary Fig. S9A and S9B). Because TPA mainly induces ROS formation in the skin indirectly through promotion of inflammation, we treated 308 keratinocytes with the ROS inducer menadione. This treatment strongly increased the levels of intracellular ROS and promoted apoptosis and reduced cell viability. These detrimental effects were partially rescued by treatment with the Nrf2-activating compounds sulforaphane or tBHQ (Fig. 6A–C; Supplementary Fig. S9C and S9D). Importantly, the protective effect of Nrf2 was strongly reduced in the presence of the G6pdx inhibitor dehydroepiandrosterone (DHEA; Fig. 6D and Supplementary Fig. S9E), which concomitantly reduced NADPH levels (Supplementary Fig. S9F). This was confirmed with the G6pdx and Pgd inhibitor 6-aminonicotinamide (6AN; Fig. 6E). This finding as well as the upregulation of PPP enzymes by Nrf2-activating compounds (Supplementary Fig. S7F) demonstrate that the activation of PPP enzymes and concomitant escape from cell death due to NADPH production also operates in *h-ras* mutated keratinocytes. In K14-HPV8/K5cre-caNrf2 mice, there was no obvious difference in the number of apoptotic keratinocytes compared with controls (Supplementary Fig. S9G), but a few cells in areas of local inflammation may be protected from ROS-induced apoptosis by caNrf2. Consistent with this assumption, sulforaphane treatment of primary keratinocytes from K14-HPV8 transgenic mice significantly reduced apoptotic cell number after menadione treatment (Fig. 6F).

Taken together, Nrf2 activation protects keratinocytes with oncogenic mutations from ROS damage and apoptosis through enhanced production of NADPH. This protective function likely promotes survival of cells in premalignant lesions (see working model; Fig. 6G and H).

NRF2 activation in precursor lesions of human epithelial skin cancer

To determine the relevance of our findings for human skin tumorigenesis, human foreskin keratinocytes (HFK) were treated with sulforaphane. This resulted in a significant upregulation of classical NRF2 target genes and of genes encoding the PPP and/or the NADPH-producing enzymes G6PDX, PGD, TALDO1, TKT, and ME1 (Fig. 7A–C). Similar to mouse keratinocytes, this did not affect proliferation, but significantly reduced intracellular ROS levels and the number of apoptotic cells (Fig. 7D–F).

Analysis of biopsies of precursor lesions of epithelial skin cancer (in particular actinic keratosis) revealed increased mRNA levels of the classic NRF2 target genes *NQO1* and *SRXN1* in 9 out of 14 samples (64%). This increase largely correlated with strong immunoreactivity of the lesions—in particular of keratinocytes—for NQO1 and for nuclear (activated) P-NRF2 (Fig. 7G and H). However, *NRF2* mRNA was not upregulated, suggesting a regulation of NRF2 at the protein level in these AK lesions (Fig. 7G). In almost half of these samples (44%), expression of *G6PDX*, *PGD*, *TKT*, *IDH1*, and *ME1* was also increased (Fig. 7J and K and Supplementary Table S3), suggesting similar metabolic alterations in precancerous lesions with NRF2 activation as observed in mice with a genetic Nrf2 activation.

Discussion

NRF2 activation is a promising strategy for chemoprevention of cancer, and natural and synthetic NRF2-activating compounds are in clinical trials for cancer prevention in high-risk patients (9). The efficacy of these activators is supported by several preclinical studies. In the skin, for example, topical sulforaphane treatment of mice reduced chemically- and UV-induced tumor formation (5, 8, 35). This is consistent with the tumor-preventive effect of caNrf2 observed in the DMBA/TPA model. However, the effect was weaker than with sulforaphane, possibly due to selective activation of Nrf2 in keratinocytes and not in the stroma. Furthermore, sulforaphane may have additional, Nrf2-independent effects. The tumor-preventive function of Nrf2 results from its potent effect on ROS and xenobiotic detoxification, which is particularly relevant in the DMBA/TPA model. Moreover, we detected Nrf2-mediated upregulation of NADPH-producing enzymes in keratinocytes, which were identified earlier as direct transcriptional targets of Nrf2 (36–39). This provides an obvious explanation for the increase in NADPH levels in the epidermis of caNrf2 transgenic mice. Furthermore, ATP levels were increased, most likely as an indirect consequence of increased PPP activity. This contributes to the chemopreventive and antioxidant functions of Nrf2, since NADPH is a redox equivalent supplier, and since ATP is consumed by several enzymes involved in ROS and xenobiotic detoxification.

Although all these studies support the usefulness of NRF2-activating compounds for cancer prevention, potential protumorigenic activities of NRF2 should not be neglected. Thus, we show here that genetic Nrf2 activation in keratinocytes has an overlapping tumor-promotive activity, whose relevance depends on the

(*Continued.*) Mean expression levels in healthy donors were set to 1. H, H&E staining (top) and IHC staining for NQO1 (middle) and P-NRF2 (Ser-40; bottom) on sections of skin cancer precursor lesions. The insets in the bottom panel show a central part of the picture at higher magnification. Note weak (left) or strong (right) NQO1 and P-NRF2 staining of keratinocytes in two different AK biopsies with low or high *NQO1* RNA expression. Dotted lines, boundary between epidermis and dermis. Scale bar, 100 μm. J, qRT-PCR for *G6PDX*, *PGD*, *TKT*, *TALDO1*, *IDH1*, and *ME1* relative to *GAPDH* using RNA from skin of healthy donors ($N = 5$ biopsies) and from patients with skin cancer precursor lesions ($N = 11/14$ biopsies). K, expression level of *G6PDX* versus *NQO1* (left graph) and *IDH1* versus *NQO1* (right graph) in precursor lesions ($N = 14$). AK biopsies with strong expression of all genes (Supplementary Table S3) are marked in red.

Published OnlineFirst November 3, 2015; DOI: 10.1158/0008-5472.CAN-15-0614

cancer model. It seems most likely that the cytoprotective activities, which reduce the accumulation of mutations, also protect any mutated cells from ROS-induced cell death, resulting in their survival and subsequent tumor formation. The observed metabolic alterations directly contribute to this protective function. Consistent with this assumption, lung epithelial cancer cell lines carrying NRF2-activating mutations have a higher proliferative activity due to upregulation of PPP enzymes (39), and transcriptional activation of Nrf2 by K-Ras and B-Raf oncoproteins increased proliferation and survival of pancreatic and lung cancer cells (40). These findings explain why activation of NRF2 in cancer cells correlates with increased malignancy and poor prognosis (9).

The consequences of these Nrf2 activities for the progression of premalignant lesions are, however, largely unexplored. Nrf2 activation is of particular importance at this stage because cells with an oncogenic *h-ras* or *c-myc* mutation are sensitive to stress-induced apoptosis because of increased ROS levels and reduced expression of antiapoptotic proteins (33, 34, 41). It seems likely that Nrf2 activation reduces the stress sensitivity of these early tumor cells. This is supported by our findings demonstrating a slight reduction in keratinocyte apoptosis in DMBA/TPA-treated K5cre-caNrf2 mice and protection of cultured keratinocytes with *h-ras* mutation from ROS-induced apoptosis by sulforaphane that was dependent on the activity of PPP enzymes. A reduction in apoptosis was also observed in sulforaphane-treated keratinocytes of K14-HPV8 transgenic mice after menadione stimulation, suggesting a similar mechanism during virus-induced tumorigenesis. These data provide evidence for a protumorigenic effect of activated Nrf2 during the cancer promotion phase by prevention of ROS-induced apoptosis of keratinocytes with oncogenic mutations.

The identified Nrf2-induced metabolic alterations are reminiscent to the metabolic reprogramming of established neoplastic cells, an important hallmark of cancer (42). It is commonly accepted that such alterations are acquired as a consequence of mutations in oncogenes and tumor suppressor genes during a long-term multistep process (43). In the presence of activated Nrf2, however, the metabolism of normal keratinocytes appears to be permanently shifted to a cancer cell-like state, creating a metabolic preconditioning, which may reduce the number of additional alterations required for complete cellular transformation and thus acceleration of tumor development. During chemical carcinogenesis, the opposing activities of Nrf2—protection from DMBA- and ROS-induced DNA mutations, but survival of cells with oncogenic mutations—are counterbalanced, resulting in a minor reduction in tumor incidence and multiplicity (Fig. 6G). In the HPV8 model, however, xenobiotic detoxification is not required, and ROS detoxification is less important due to a lower level of inflammation. As a consequence, the effect of Nrf2 on survival of cells with oncogenic mutations predominates in K14-HPV8 mice, resulting in a strong increase in tumor incidence in the presence of activated Nrf2 (Fig. 6H). Therefore, the effect of Nrf2 on skin tumorigenesis is dependent on the tumor model.

The results obtained in this study are of obvious importance for human skin carcinogenesis, since we found a strong staining for NQO1 and P-NRF2 in keratinocytes and upregulation of classical NRF2 target genes and genes encoding PPP enzymes in a subset of biopsies from patients with precancerous skin lesions. Although these results need to be confirmed with a larger number of patients, they suggest that NRF2 activation occurs in these early lesions. This is likely to result in metabolic changes that promote keratinocyte survival, similar to our mouse models after genetic Nrf2 activation. In the future, it will be interesting to determine the mechanisms of NRF2 activation in precancerous skin lesions.

Taken together, our results unraveled an unexpected protumorigenic activity during the promotion phase by protecting premalignant cells from stress-induced apoptosis. Therefore, the outcome of NRF2 activation critically depends on the stage of tumorigenesis and most likely also on the etiologic agent and duration of NRF2 activation. Therefore, the benefits of NRF2 activation should be considered in light of the here described protumorigenic activities.

Disclosure of Potential Conflicts of Interest

No potential conflicts of interest were disclosed.

Authors' Contributions

Conception and design: R. Dummer, S. Werner, M. Schafer
Development of methodology: D. Hohl
Acquisition of data (provided animals, acquired and managed patients, provided facilities, etc.): F. Rolfs, M. Huber, A. Kuehne, S. Kramer, E. Haertel, S. Muzumdar, J. Wagner, Y. Tanner, F. Bohm, N. Zamboni, M.P. Levesque, R. Dummer, H.-D. Beer, D. Hohl, M. Schafer
Analysis and interpretation of data (e.g., statistical analysis, biostatistics, computational analysis): F. Rolfs, A. Kuehne, S. Kramer, E. Haertel, S. Muzumdar, J. Wagner, Y. Tanner, F. Bohm, S. Smola, D. Hohl, S. Werner, M. Schafer
Writing, review, and/or revision of the manuscript: F. Rolfs, S. Smola, R. Dummer, S. Werner, M. Schafer
Administrative, technical, or material support (i.e., reporting or organizing data, constructing databases): D. Hohl
Study supervision: S. Werner, M. Schafer
Other (metabolomics): A. Kuehne

Acknowledgments

The authors thank Christiane Born-Berclaz, Nadja Bain, Nicole Hallschmid, Hayley Hiebert, and Mario Gysi for excellent technical assistance, Dr. Tamara Ramadan, Eva Gleißner, Asim Sengör, and Alain Leonid Haeller (all from ETH Zurich) for invaluable experimental help, Prof. Uwe Sauer (ETH Zurich) for invaluable support, Prof. Herbert Pfister (University of Cologne, Germany) for K14-HPV8 mice, Dr. Patrizia Stoitzner (University of Innsbruck, Austria) for the anti-CD207 antibody, and Dr. Stefan Zoller, Catharine Aquino, and Dr. Hubert Rehrauer (Functional Genomics Center Zurich) for help with the microarray experiments.

Grant Support

This work was supported by grants from the Wilhelm Sander-Stiftung (S. Werner), Cancer Research Switzerland (KFS 2822-08-2011 to S. Werner), and the Swiss National Science Foundation (310030_132884 to S. Werner and 31003A-138416 to M. Huber).

The costs of publication of this article were defrayed in part by the payment of page charges. This article must therefore be hereby marked *advertisement* in accordance with 18 U.S.C. Section 1734 solely to indicate this fact.

Received March 9, 2015; revised August 13, 2015; accepted August 19, 2015; published OnlineFirst November 3, 2015.

References

1. Sander CS, Chang H, Hamm F, Elsner P, Thiele JJ. Role of oxidative stress and the antioxidant network in cutaneous carcinogenesis. Int J Dermatol 2004;43:326–35.
2. Suzuki T, Motohashi H, Yamamoto M. Toward clinical application of the Keap1-Nrf2 pathway. Trends Pharmacol Sci 2013;34:340–6.

3. Schäfer M, Dütsch S, auf dem Keller U, Navid F, Schwarz A, Johnson DA, et al. Nrf2 establishes a glutathione-mediated gradient of UVB cytoprotection in the epidermis. Genes Dev 2010;24:1045–58.
4. Kawachi Y, Xu X, Taguchi S, Sakurai H, Nakamura Y, Ishii Y, et al. Attenuation of UVB-induced sunburn reaction and oxidative DNA damage with no alterations in UVB-induced skin carcinogenesis in Nrf2 gene-deficient mice. J Invest Dermatol 2008;128:1773–9.
5. Xu C, Huang MT, Shen G, Yuan X, Lin W, Khor TO, et al. Inhibition of 7,12-dimethylbenz(a)anthracene-induced skin tumorigenesis in C57BL/6 mice by sulforaphane is mediated by nuclear factor E2-related factor 2. Cancer Res 2006;66:8293–6.
6. auf dem Keller U, Huber M, Beyer TA, Kumin A, Siemes C, Braun S, et al. Nrf transcription factors in keratinocytes are essential for skin tumor prevention but not for wound healing. Mol Cell Biol 2006;26:3773–84.
7. Saw CL, Huang MT, Liu Y, Khor TO, Conney AH, Kong AN. Impact of Nrf2 on UVB-induced skin inflammation/photoprotection and photoprotective effect of sulforaphane. Mol Carcinog 2011;50:479–86.
8. Dinkova-Kostova AT, Jenkins SN, Fahey JW, Ye L, Wehage SL, Liby KT, et al. Protection against UV-light-induced skin carcinogenesis in SKH-1 high-risk mice by sulforaphane-containing broccoli sprout extracts. Cancer Lett 2006;240:243–52.
9. Sporn MB, Liby KT. NRF2 and cancer: the good, the bad and the importance of context. Nat Rev Cancer 2012;12:564–71.
10. Jaramillo MC, Zhang DD. The emerging role of the Nrf2-Keap1 signaling pathway in cancer. Genes Dev 2013;27:2179–91.
11. Lawrence MS, Stojanov P, Mermel CH, Robinson JT, Garraway LA, Golub TR, et al. Discovery and saturation analysis of cancer genes across 21 tumour types. Nature 2014;505:495–501.
12. Kim YR, Oh JE, Kim MS, Kang MR, Park SW, Han JY, et al. Oncogenic NRF2 mutations in squamous cell carcinomas of oesophagus and skin. J Pathol 2010;220:446–51.
13. Schaper ID, Marcuzzi GP, Weissenborn SJ, Kasper HU, Dries V, Smyth N, et al. Development of skin tumors in mice transgenic for early genes of human papillomavirus type 8. Cancer Res 2005;65:1394–400.
14. Schäfer M, Farwanah H, Willrodt AH, Huebner AJ, Sandhoff K, Roop D, et al. Nrf2 links epidermal barrier function with antioxidant defense. EMBO Mol Med 2012;4:362–79.
15. Buescher JM, Moco S, Sauer U, Zamboni N. Ultrahigh performance liquid chromatography-tandem mass spectrometry method for fast and robust quantification of anionic and aromatic metabolites. Anal Chem 2010;82:4403–12.
16. Fuhrer T, Heer D, Begemann B, Zamboni N. High-throughput, accurate mass metabolome profiling of cellular extracts by flow injection-time-of-flight mass spectrometry. Anal Chem 2011;83:7074–80.
17. Wishart DS, Jewison T, Guo AC, Wilson M, Knox C, Liu Y, et al. HMDB 3.0–The Human Metabolome Database in 2013. Nucleic Acids Res 2013;41:D801–7.
18. Abel EL, Angel JM, Kiguchi K, DiGiovanni J. Multi-stage chemical carcinogenesis in mouse skin: fundamentals and applications. Nat Protoc 2009;4:1350–62.
19. Schäfer M, Willrodt AH, Kurinna S, Link AS, Farwanah H, Geusau A, et al. Activation of Nrf2 in keratinocytes causes chloracne (MADISH)-like skin disease in mice. EMBO Mol Med 2014;6:442–57.
20. Zhang L, Jin Y, Huang M, Penning TM. The role of human Aldo-Keto reductases in the metabolic activation and detoxication of polycyclic aromatic hydrocarbons: interconversion of PAH catechols and PAH o-Quinones. Front Pharmacol 2012;3:193.
21. Long DJ III, Waikel RL, Wang XJ, Roop DR, Jaiswal AK. NAD(P)H:quinone oxidoreductase 1 deficiency and increased susceptibility to 7,12-dimethylbenz[a]-anthracene-induced carcinogenesis in mouse skin. J Natl Cancer Inst 2001;93:1166–70.
22. Modi BG, Neustadter J, Binda E, Lewis J, Filler RB, Roberts SJ, et al. Langerhans cells facilitate epithelial DNA damage and squamous cell carcinoma. Science 2012;335:104–8.
23. Wei H, Frenkel K. Relationship of oxidative events and DNA oxidation in SENCAR mice to *in vivo* promoting activity of phorbol ester-type tumor promoters. Carcinogenesis 1993;14:1195–201.
24. Pfister H. Chapter 8: Human papillomavirus and skin cancer. J Natl Cancer Inst Monogr 2003:52–6.
25. Hufbauer M, Lazic D, Akgul B, Brandsma JL, Pfister H, Weissenborn SJ. Enhanced human papillomavirus type 8 oncogene expression levels are crucial for skin tumorigenesis in transgenic mice. Virology 2010;403:128–36.
26. Marcuzzi GP, Hufbauer M, Kasper HU, Weissenborn SJ, Smola S, Pfister H. Spontaneous tumour development in human papillomavirus type 8 E6 transgenic mice and rapid induction by UV-light exposure and wounding. J Gen Virol 2009;90:2855–64.
27. Kim C, Pasparakis M. Epidermal p65/NF-kappaB signalling is essential for skin carcinogenesis. EMBO Mol Med 2014;6:970–83.
28. van Hogerlinden M, Rozell BL, Ahrlund-Richter L, Toftgard R. Squamous cell carcinomas and increased apoptosis in skin with inhibited Rel/nuclear factor-kappaB signaling. Cancer Res 1999;59:3299–303.
29. Lind MH, Rozell B, Wallin RP, van Hogerlinden M, Ljunggren HG, Toftgard R, et al. Tumor necrosis factor receptor 1-mediated signaling is required for skin cancer development induced by NF-kappaB inhibition. Proc Natl Acad Sci U S A 2004;101:4972–7.
30. Dajee M, Lazarov M, Zhang JY, Cai T, Green CL, Russell AJ, et al. NF-kappaB blockade and oncogenic Ras trigger invasive human epidermal neoplasia. Nature 2003;421:639–43.
31. Yuspa SH, Morgan DL. Mouse skin cells resistant to terminal differentiation associated with initiation of carcinogenesis. Nature 1981;293:72–4.
32. Strickland JE, Greenhalgh DA, Koceva-Chyla A, Hennings H, Restrepo C, Balaschak M, et al. Development of murine epidermal cell lines which contain an activated rasHa oncogene and form papillomas in skin grafts on athymic nude mouse hosts. Cancer Res 1988;48:165–9.
33. Irani K, Xia Y, Zweier JL, Sollott SJ, Der CJ, Fearon ER, et al. Mitogenic signaling mediated by oxidants in Ras-transformed fibroblasts. Science 1997;275:1649–52.
34. Schwieger A, Bauer L, Hanusch J, Sers C, Schafer R, Bauer G. ras oncogene expression determines sensitivity for intercellular induction of apoptosis. Carcinogenesis 2001;22:1385–92.
35. Gills JJ, Jeffery EH, Matusheski NV, Moon RC, Lantvit DD, Pezzuto JM. Sulforaphane prevents mouse skin tumorigenesis during the stage of promotion. Cancer Lett 2006;236:72–9.
36. MacLeod AK, McMahon M, Plummer SM, Higgins LG, Penning TM, Igarashi K, et al. Characterization of the cancer chemopreventive NRF2-dependent gene battery in human keratinocytes: demonstration that the KEAP1-NRF2 pathway, and not the BACH1-NRF2 pathway, controls cytoprotection against electrophiles as well as redox-cycling compounds. Carcinogenesis 2009;30:1571–80.
37. Malhotra D, Portales-Casamar E, Singh A, Srivastava S, Arenillas D, Happel C, et al. Global mapping of binding sites for Nrf2 identifies novel targets in cell survival response through ChIP-Seq profiling and network analysis. Nucleic Acids Res 2010;38:5718–34.
38. Thimmulappa RK, Mai KH, Srisuma S, Kensler TW, Yamamoto M, Biswal S. Identification of Nrf2-regulated genes induced by the chemopreventive agent sulforaphane by oligonucleotide microarray. Cancer Res 2002;62:5196–203.
39. Mitsuishi Y, Taguchi K, Kawatani Y, Shibata T, Nukiwa T, Aburatani H, et al. Nrf2 redirects glucose and glutamine into anabolic pathways in metabolic reprogramming. Cancer Cell 2012;22:66–79.
40. DeNicola GM, Karreth FA, Humpton TJ, Gopinathan A, Wei C, Frese K, et al. Oncogene-induced Nrf2 transcription promotes ROS detoxification and tumorigenesis. Nature 2011;475:106–9.
41. Tanaka H, Matsumura I, Ezoe S, Satoh Y, Sakamaki T, Albanese C, et al. E2F1 and c-Myc potentiate apoptosis through inhibition of NF-kappaB activity that facilitates MnSOD-mediated ROS elimination. Mol Cell 2002;9:1017–29.
42. Hanahan D, Weinberg RA. Hallmarks of cancer: the next generation. Cell 2011;144:646–74.
43. Cairns RA, Harris IS, Mak TW. Regulation of cancer cell metabolism. Nat Rev Cancer 2011;11:85–95.

Cancer Research
The Journal of Cancer Research (1916–1930) | The American Journal of Cancer (1931–1940)

AACR American Association for Cancer Research

Nrf2 Activation Promotes Keratinocyte Survival during Early Skin Carcinogenesis via Metabolic Alterations

Frank Rolfs, Marcel Huber, Andreas Kuehne, et al.

Cancer Res Published OnlineFirst November 3, 2015.